Structure

In This Issue

In Review: [FeFe]-Hydrogenases: Structure, Mechanism, and Maturation

PAGE 1038

Hydrogenases are key enzymes of the energy metabolism in diverse microbial communities. Based on their metal content, they are divided into three major classes, the [Fe]-, [FeFe]-, and [NiFe]-hydrogenases, which are evolutionarily unrelated but share in common similar nonprotein ligand assemblies at their active site metal centers that are not found elsewhere in biology. In this review, Mulder et al. discuss how the wealth of structural information on different classes and different states of hydrogenase enzymes have contributed to our understanding of the biochemistry of hydrogen metabolism and have created a clearer picture of the [FeFe]-hydrogenase maturation pathway.

Ubiquitin Chain Reagents

PAGE 1053

Free ubiquitin chains are key tools for studying the molecular interactions that underlie ubiquitin-signaling pathways. However, the production of high-quality ubiquitin chain reagents at the multimilligram levels required for detailed biophysical/structural analysis has been challenging despite experimental precedent. Here, Dong et al. provide a detailed and practical road map for producing linear, K11-, K48-, and K63-linked ubiquitin chains of sufficient yield and purity for these kinds of studies as well as for generating and applying novel ubiquitin reagents.

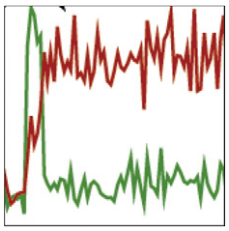

Strand Exchange by RecA in Real Time

PAGE 1064

RecA protein plays a critical role in double strand break repair in *E. coli*. RecA binds to single strand DNA to form a helical filament that mediates homology search and catalyzes basepair exchange with a homologous double strand DNA. Ragunathan et al. developed a single molecule fluorescence based assay with a few base pair and milliseconds resolution to understand this complex multistep process. Their model proposes that RecA-mediated strand exchange proceeds by concomitantly destabilizing and exchanging complementary base pairs in 3 bp increments, while the displaced DNA, which is transiently bound to the RecA filament, displays extensive dynamic behavior prior to its dissociation.

Death Signaling Switch in Apaf-1

PAGE 1074

The apoptotic protease-activating factor 1 (Apaf-1) relays the death signal in the mitochondrial pathway of apoptosis. Apaf-1 oligomerizes upon binding of mitochondrially released cytochrome *c* into the heptameric apoptosome complex to ignite the downstream cascade of caspases. Reubold et al. present here the 3.0 Å crystal structure of full-length murine Apaf-1 in the absence of cytochrome *c*. It shows how the mammalian death switch is kept in its "off" position. By comparing the "off" state with Apaf-1 in its apoptosomal conformation, they depict the molecular events that transform Apaf-1 from auto-inhibited monomer to a building block of the caspase-activating apoptosome.

Apoptosome Activation

PAGE 1084

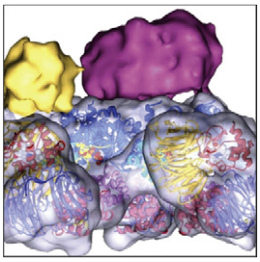

Activation of procaspase-9 (pc-9) on the apoptosome is a pivotal step in the intrinsic cell death pathway. Here, Yuan et al. have defined a "proximity-induced association" mechanism for pc-9 activation, in which 5–7 pc-9 zymogens bind to the apoptosome to create a disk comprised of pc-9 and Apaf-1 CARDs. This disk with flexibly tethered catalytic domains sits above the apoptosome and is located off-center relative to the central hub. This mismatch and the size of the disk may allow only a single pc-9 catalytic domain to bind to the central hub, where it is activated by a local conformational change.

Structural Basis of Anti-VEGF Receptor Antibody Function

PAGE 1097

Inhibition of angiogenesis is key to treating many diseases, from macular degeneration to cancer. Some anticancer therapies disrupt the angiogenic signaling pathway involving vascular endothelial growth factors (VEGFs) and their receptors, in particular, VEGF receptor 2, or KDR. IMC-1121B is a fully human antibody targeting KDR. The structure of the Fab fragment of IMC-1121B in complex with domain 3 of KDR presented here by Franklin et al. reveals the mechanism by which this antibody inhibits KDR signaling. As the antibody prevents all VEGF family ligands from receptor binding, it has great promise as a broadly effective antiangiogenic cancer therapy.

GPCR Dock 2010 Assessment

PAGE 1108

The community-wide GPCR Dock assessment is conducted to evaluate the status of molecular modeling and docking for human G protein-coupled receptors. Kufareva et al. present the results of the current round that featured three targets of varying modeling difficulty. Thirty five groups submitted 275 complex structure predictions prior to release of X-ray coordinates. For the target with abundant biochemical data and 35%–40% homology to the existing structures, the best predictions captured complex details at the atomic resolution level; however, modeling by more distant homology remained challenging. The results provide guidance for modelers and crystallographers in facilitating structural coverage of the GPCR universe.

Dynamics of p110δ Regulation

PAGE 1127

The class IA family of phosphoinositide 3-kinases (PI3K) are kept in a tightly inhibited state by their regulatory subunits, and this inhibition can be relieved by binding to phosphorylated receptor tyrosine kinases (RTKs). Burke et al. used deuterium exchange mass spectrometry to study the dynamics of this regulation for the p110δ isoform of PI3K. Both the presence of the p85 subunit and binding to RTK phosphopeptides regulates the affinity of PI3K for membrane vesicles. Although all class IA PI3Ks are regulated by p85 subunits, the p110δ and p110α catalytic subunits are differentially regulated by the cSH2 domain of p85.

CCL5 Assembly into Higher Order Structures

PAGE 1138

CCL5 (RANTES) is a proinflammatory chemokine known to activate leukocytes through its receptor CCR5. Monomeric CCL5 initiates certain signaling events, but in vivo migration of leukocytes depends on higher order aggregates and interaction with glycosaminoglycans. Although dimeric structures of CCL5 exist, structures of higher order aggregates have not been reported. An integrated approach by Wang et al. using NMR, SAXS, and hydroxyl radical footprinting has now produced a structural model for the assembly of dimeric units of CCL5 into higher order oligomers, which shows an extended GAG binding site and a receptor interaction interface that may facilitate cell migration.

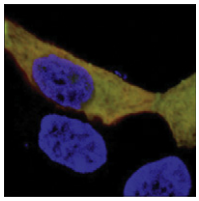

AMSH Recruitment by ESCRT-III CHMP3

PAGE 1149

Endosomal sorting complexes required for transport (ESCRT) recognize ubiquitinated cargo and catalyze diverse budding processes. The deubiquitinating enzyme AMSH associates with ESCRT-0 and ESCRT-III to regulate ubiquitin turnover. The crystal structure of an N-terminal fragment of AMSH in complex with ESCRT-III CHMP3 reported by Solomons et al. reveals an elongated 90 Å long helical assembly that interacts with a C-terminal helical region of CHMP3. They also find a regulatory role of the first helix of AMSH during HIV-1 budding. These results indicate a tight coupling of ESCRT-III CHMP3 and AMSH functions and provide novel insight into the regulation of ESCRT-III.

Structural Basis of Charcot-Marie-Tooth Disease

PAGE 1160

Mutations in peripheral myelin protein 22 (PMP22) can result in the common peripheral neuropathy Charcot-Marie-Tooth disease (CMTD). The Leu16Pro mutation in PMP22 results in misassembly of the protein, which causes the Trembler-J (TrJ) disease phenotype. Here, Sakakura et al. elucidate the structural defects present in TrJ PMP22. They observe that this disease mutation results in profound changes in the conformation and dynamics of the normally helical first transmembrane segment of this tetraspan membrane protein. This destabilizes the folded state in favor of a state where transmembrane helices 2–4 form a molten globular structure, from which transmembrane helix 1 (TM1) is dissociated.

Anti-HIV Activity of OAA Revealed

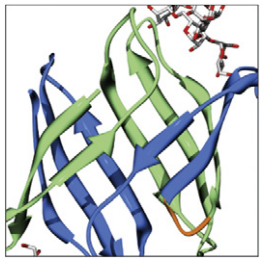

PAGE 1170

The cyanobacterial *Oscillatory Agardhii* agglutinin (OAA) is a recently discovered HIV-inactivating lectin that interacts with high-mannose sugars. Koharudin and Gronenborn show by NMR spectroscopy that α3,α6-mannopentaose binds to OAA tightly and specifically at two binding sites with identical affinities. Atomic details of the specific protein-sugar contacts in the recognition loops of OAA were delineated in the high-resolution crystal structures of free and glycan-complexed protein. These combined NMR and crystallographic results provide structural insights into the mechanism by which OAA specifically recognizes the branched Man-9 core, distinct from the recognition of the nonreducing end of high-mannose carbohydrates by other antiviral lectins.

Predicting Protein Structure through Contact Predictions

PAGE 1182

Although residue-residue contact maps dictate topology of proteins, sequence-based ab initio contact predictions have been found little use in structure prediction due to their low accuracy. Wu et al. developed a composite set of nine SVM-based contact predictors, which are used in I-TASSER simulation in combination with sparse template contact restraints. They demonstrate that remarkable improvements of I-TASSER models can be achieved by contact predictions for both easy and hard targets. In several cases, contact predictions essentially convert "nonfoldable" targets into "foldable" ones. These findings suggest avenues to improve the accuracy of protein structure prediction, especially for free-modeling targets.

Flexible Architecture of IP_3R1 by Cryo-EM

PAGE 1192

Using single particle electron cryomicroscopy, Ludtke et al. have solved the high-resolution structure of a fully functional type 1 Inositol 1,4,5-trisphosphate receptor (IP_3R1) from cerebellum in the closed state. Several helices in the membrane-spanning region have been resolved, permitting them to establish a connection with the structure of K^+ channels. This study demonstrates that these distantly related channels exhibit architectural similarities in the outer pore region, which in the case of IP_3R1 is the endoplasmic mouth of the channel pore. This work thus resolves the debates regarding the structure of IP_3R1 and forms the basis of future studies.

